

Decoherence vs entanglement in coined quantum walks

Olivier Maloyer^{1,2} and Viv Kendon^{2,*}

¹*Magistère de Physique Fondamentale d'Orsay, Université Paris-Sud, Orsay, France*

²*School of Physics and Astronomy, University of Leeds, LS2 9JT, United Kingdom.*

(Dated: December 29th, 2006)

Quantum versions of random walks on the line and cycle show a quadratic improvement in their spreading rate and mixing times respectively. The addition of decoherence to the quantum walk produces a more uniform distribution on the line, and even faster mixing on the cycle by removing the need for time-averaging to obtain a uniform distribution. We calculate numerically the entanglement between the coin and the position of the quantum walker and show that the optimal decoherence rates are such that all the entanglement is just removed by the time the final measurement is made.

Contents

I. Introduction and background	1
A. Simple, coined, quantum walks	2
B. Decoherence model	4
C. Decoherence in the walk on the line	5
D. Decoherence in the walk on a cycle	5
E. Entanglement in mixed states	6
II. Results	7
A. Entanglement in the walk on the line	8
B. Entanglement in the walk on a cycle	9
C. Conclusion	10
Acknowledgments	10
References	10

I. INTRODUCTION AND BACKGROUND

Simple quantum generalisations of classical random walks spread quadratically faster on the line [1, 2], and mix quadratically faster on the cycle [3]. These promising examples of a quantum speed up were soon followed by several algorithms based on quantum walks. Shenvi et al [4] proved a quantum walk can solve the unsorted database search problem quadratically faster, and Childs et al [5] proved an exponential speed up for crossing a particular type of graph. Several more algorithms have followed these, Ambainis [6] gives an overview of quantum walk algorithms, and Kempe [7] provides an introductory review of quantum walks and their properties. Physical implementations of quantum walks have also been proposed [8, 9, 10], as sensitive tests of coherent control over

*Electronic address: V.Kendon@leeds.ac.uk

quantum particles. Optical implementation dates back to Bouwmeester et al. [11], which can be viewed as a quantum walk on the line with many photons, as Kendon and Sanders [12] explain. A quantum walk on a cycle with four nodes has been implemented on a NMR quantum computer using three qubits, two for the position label and one for the coin [13].

Quantum walks on simple one-dimensional structures remain a fertile testing ground for further research. It was shown numerically by Kendon and Tregenna [14] that the addition of decoherence or measurements to the quantum walk dynamics can optimise the spreading and mixing properties for quantum walks on both the line and the cycle (recently proved by Richter [15, 16]). A detailed survey of the effects of decoherence in quantum walks can be found in [17]. In this work we look closely at how the interplay between quantum evolution and decoherence or measurements produces optimal computational properties. In particular, we calculate the entanglement between the coin and the position of the quantum walker and observe how it varies as the quantum walk evolution unfolds. This study is restricted to quantum walks taking place in discrete time and space, using a quantum coin to control the choice of direction. Thus we can use the entanglement between the coin and position as an indication of how “quantum” the walk is as it progresses. A different method for assessing “quantumness” would be needed for continuous-time quantum walks (introduced for quantum algorithms by Farhi and Gutmann [18]).

In the following subsections we describe the background material: simple quantum walks, the decoherence model we use, and the entanglement measure (negativity) we employed. The results of our study are then described in §II, first for the line, then for cycles, and finally a summary of the common elements of our findings.

A. Simple, coined, quantum walks

A discrete-time (coined) quantum walk dynamics consists of a quantum “coin toss” operation **C**, followed by a shift operation **S** to move the quantum walker to a new position. These are repeated alternately for T steps of the quantum walk, and the final position of the quantum walker is measured. For quantum walks on the line and the cycle, we have just two choices of which way to step, so the quantum coin is a two state system. We write $|x, c\rangle$ for a quantum walker at position x with a coin in state $c \in \{+1, -1\}$. For a walk on the line, $x \in \mathbb{Z}$ and for a walk on a cycle of size N , we have $x \in \mathbb{Z}_N$. A classical random walk can only occupy one location at any given time, but a quantum walker can be in a superposition of different locations. The full state of the quantum walk $|\Psi(t)\rangle$ at time t can be written as a combination of terms in each basis state $|x, c\rangle$,

$$|\Psi(t)\rangle = \sum_{x,c} \psi_{x,c}(t) |x, c\rangle, \quad (1)$$

where $\psi_{x,c}(t) \in \mathbb{C}$ and the normalisation is $\sum_{x,c} |\psi_{x,c}(t)|^2 = 1$. When the quantum walk is measured (in the basis just defined), the walker is found in a single location with a definite coin state. The probability of finding the quantum walker at position y with the coin in state b is given by

$$P(y, b, t) = |\langle y, b | \Psi(t) \rangle|^2 = |\psi_{y,b}(t)|^2 \quad (2)$$

since the basis states are orthogonal, $\langle y, b | x, c \rangle = \delta_{xy} \delta_{bc}$.

The coin toss **C** and shift **S** are defined in terms of their action on the basis states $|x, c\rangle$,

$$\mathbf{S}|x, c\rangle = |x + c, c\rangle \quad (3)$$

$$\mathbf{C}|x, c\rangle = (|x, -c\rangle + c|x, c\rangle)/\sqrt{2} \quad (4)$$

One can add more general bias or phase into the coin toss operation, see, for example, [19], but this does not greatly change the basic properties of the quantum walk on a line or cycle, so we will consider only the unbiased case in this paper. For a quantum walk starting at position $x = 0$ with the coin in a superposition state $(|-1\rangle + i|+1\rangle)/\sqrt{2}$, (where $i = \sqrt{-1}$) we can write a quantum walk of T steps as

$$|\Psi(T)\rangle = (\mathbf{SC})^T \{|0, -1\rangle + i|0, +1\rangle\} / \sqrt{2} \quad (5)$$

The solution for $|\Psi(T)\rangle$ may be obtained by various methods such as Fourier analysis [2] and path counting [1], and has been studied extensively. The key result is that spreading on the line proceeds linearly with the number of time steps. We can use the standard deviation $\sigma_Q(T)$ of the probability distribution to quantify the spreading rate. For a quantum walk on the line,

$$\sigma_Q(T) = \sum_{x,c} x^2 P(x, c, T) \simeq \left(1 - \frac{1}{\sqrt{2}}\right)^{1/2} T, \quad (6)$$

asymptotically in the limit of large T [2]. In contrast, for the classical random walk, the standard deviation is $\sigma_C(T) = \sqrt{T}$.

On the cycle, we are interested in mixing times rather than spreading. Mixing times can be defined in a number of different ways, we choose the main definition given in [3],

$$M(\epsilon) = \min \{T \mid \forall t > T : \|P(x, t) - P_u\|_{\text{tv}} < \epsilon\} \quad (7)$$

where P_u is the limiting distribution over the cycle, and the total variational distance (TVD) is defined as

$$\|P(x, T) - P_u\|_{\text{tv}} \equiv \sum_x |P(x, T) - P_u|. \quad (8)$$

A classical random walk on the cycle mixes to within ϵ of the uniform distribution in time proportional to $N^2 \log(1/\epsilon)$, where ϵ can be chosen arbitrarily small.

Pure quantum walks, on the other hand, do not mix to a stationary distribution. Their deterministic dynamics ensures they continue to oscillate indefinitely. There are several ways to obtain mixing behaviour, first explored by Aharonov et al [3]. By defining a time-averaged probability distribution for the quantum walk,

$$\overline{P(x, c, T)} = \sum_{t=0}^{T-1} P(x, c, t) \quad (9)$$

they proved that $\overline{P(x, c, T)}$ does converge to a stationary distribution on a cycle, and that on odd-sized cycles the stationary distribution is uniform. A mixing time can be defined for $\overline{P(x, c, T)}$,

$$\overline{M}(\epsilon) = \min \left\{ T \mid \forall t > T : \|\overline{P(x, c, t)} - P_u\|_{\text{tv}} < \epsilon \right\}. \quad (10)$$

and Aharonov et al [3] proved that, for odd-sized cycles, $\overline{M}(\epsilon)$ is bounded above by $O(\epsilon^{-3} N \log N)$, almost quadratically faster (in N) than a classical random walk. Kendon and Tregenna [14],

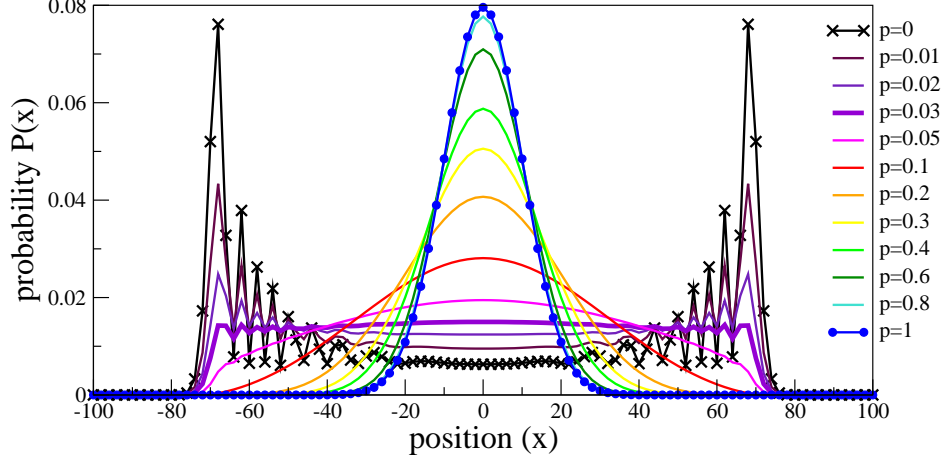


FIG. 1: Numerical data for a quantum walk on the line of 100 steps, with decoherence applied to both the coin and position, for various decoherence rates between zero (quantum) and one (classical) as shown in the key.

observed numerically that $\overline{M}(\epsilon) \sim O(N/\epsilon)$, this has been recently confirmed analytically by Richter [16].

Notice that we pay a price for our time-averaging: the scaling with the precision ϵ is now linear instead of logarithmic. Aharonov et al [3] provide a fix for this in the form of a “warm start”. The quantum walk is run several times, each repetition starting from the final state of the previous run. A small number of such repetitions is sufficient to reduce the scaling of the mixing time $\overline{M}(\epsilon)$ to logarithmic in ϵ .

Both the quantum walk on the line and the cycle thus provide a quadratic speed up over classical random walks. This quadratic speed up does not carry over to all quantum walks on higher dimensional structures, see, for example, [20, 21, 22]. It remains an open question how ubiquitous this behaviour really is.

B. Decoherence model

We will consider decoherence in the form of randomly-occurring uncorrelated non-unitary events added to the quantum walk dynamics already described. The evolution of the quantum walk must now be described using a density operator $\rho(t)$ given by

$$\rho(t+1) = (1-p)\mathbf{S}\mathbf{C}\rho(t)\mathbf{C}^\dagger\mathbf{S}^\dagger + p\sum_j \mathbb{P}_j\mathbf{S}\mathbf{C}\rho(t)\mathbf{C}^\dagger\mathbf{S}^\dagger\mathbb{P}_j^\dagger. \quad (11)$$

Here \mathbb{P}_j is a projection that represents the action of the non-unitary decoherence events and p is the probability of applying the decoherence per time step, or, completely equivalent mathematically, to a weak coupling between the quantum walk system and a Markovian environment with coupling strength p . For a pure state, the density operator $\rho(t) \equiv |\Psi(t)\rangle\langle\Psi(t)|$, it thus has the normalisation $\text{Tr}[\rho(t)] = 1$. For $p = 0$, equation (11) reduces to the pure quantum walk described in §IA, and for $p = 1$, to a classical random walk.

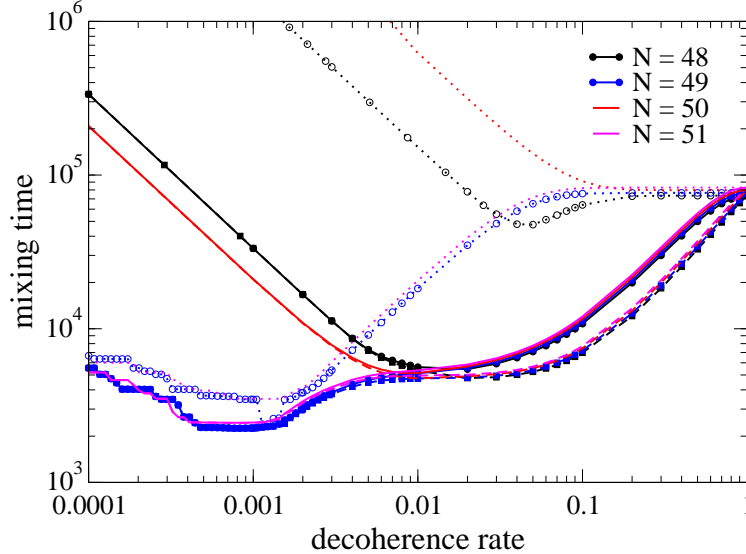


FIG. 2: Numerical data for the time-averaged mixing time $\overline{M}_\epsilon(p)$ on cycles of size $N = 48$, $N = 49$, $N = 50$ and $N = 51$, for coin (dotted), position (dashed) and both (solid) subject to decoherence, using $\epsilon = 0.002$.

C. Decoherence in the walk on the line

Full analytical solution of a non-unitary quantum walk has been done only for a few special cases. For quantum walks on the line, Brun et al [23] analysed the case of random measurements on the coin only. While analytical solution is challenging, equation (11) lends itself readily to numerical simulation since ρ , \mathbf{S} and \mathbf{C} can be manipulated as complex matrices, while the \mathbb{P}_j generally remove some or all of the off-diagonal entries in ρ . Kendon and Tregenna [14] evolved equation (11) numerically for various choices of \mathbb{P}_j : projection onto the position space, projection onto the coin space, and projection of both coin and position. In all cases, the spreading rate is reduced, in the long time limit [23], it becomes proportional to \sqrt{T} instead of proportional to T . More interesting behaviour is seen for intermediate times and decoherence rates p with decoherence applied to the position, or to both the position and coin. Kendon and Tregenna observed that, for $2 \lesssim pT \lesssim 5$, the distribution becomes very close to uniform while retaining the full quantum linear spreading rate, see figure 1. With decoherence applied to the coin only, the distribution retains a cusp shape [14]. To quantify this the TVD given by equation (8) can be used, this time with P_u defined to be a top-hat of appropriate width $x \in \{\pm T/\sqrt{2}\}$, see [1, 2]. Since the quantum walk (in common with the classical random walk on which it is based) has the property that at odd(even) time steps the walker will only be found at odd(even)-numbered locations, the top-hat definition of P_u also incorporates this property.

D. Decoherence in the walk on a cycle

For a quantum walk on the cycle subjected to Markovian decoherence, the mixing behaviour is dramatically improved if the decoherence is applied to the position. Decoherence guarantees mixing to the uniform distribution, and a similar judicious choice of $2 \lesssim pN \lesssim 5$ produces a minimum

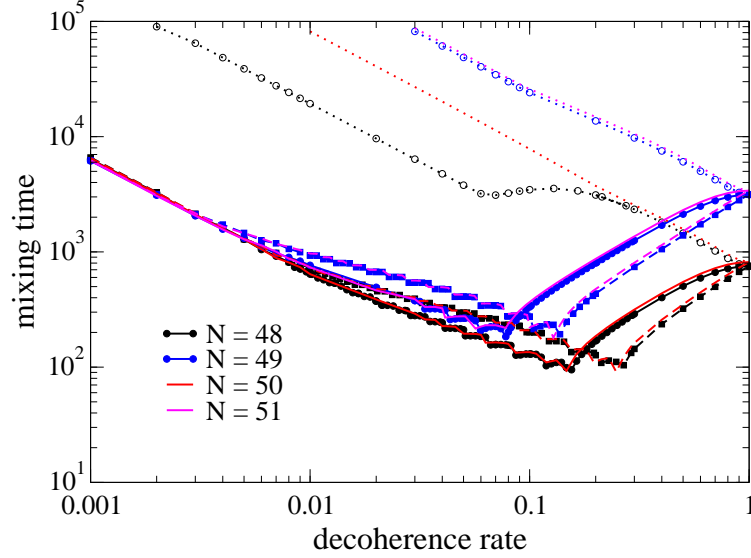


FIG. 3: Numerical data for the mixing time, without time-averaging, $M_\epsilon(p)$ on cycles of size $N = 48$ to $N = 51$, for decoherence applied to coin only (dotted), position only (dashed) and both (solid), using $\epsilon = 0.002$.

mixing time [14], well below the classical value. Decoherence applied only to the coin does cause the quantum walk on a cycle to mix, but not significantly faster than a classical random walk. Furthermore, time-averaging is no longer necessary, mixing occurs in time $O(N \log(1/\epsilon))$. This has recently been proved by Richter [16]. This mixing behaviour is illustrated in figures 2 and 3 for cycles of size 48, 49, 50 and 51. Figure 2 shows time-averaged mixing times while figure 3 shows mixing times without any time averaging. Note the scales are different between the two figures, the mixing times are longer when time-averaging is applied, reflecting the change from logarithmic to linear dependence on $1/\epsilon$.

E. Entanglement in mixed states

Quantum walks with decoherence on the line and the cycle thus provide two examples where the optimal computational properties are obtained for a judicious combination of quantum dynamics and decoherence. In order to investigate this phenomenon in more detail, we asked how “quantum” the system is by the end of the quantum walk when the optimal amount of decoherence is applied. To quantify this, we looked at the entanglement, which is a property that depends on the quantum correlations in the system.

We chose our entanglement measure to be the negativity [24, 25, 26] because this can be calculated numerically in a fairly straightforward manner for density operators such as $\rho(t)$, and there are few options that meet this criterion. First we must choose a division of our system into two (or more) subsystems between which to identify the entanglement. For our quantum walk, the natural division is between the coin and the quantum walker’s position. We note that the entanglement across this division will be the same whether we regard the quantum walk as a physical system with a qubit coin and a unary position, or as an algorithm running on a quantum

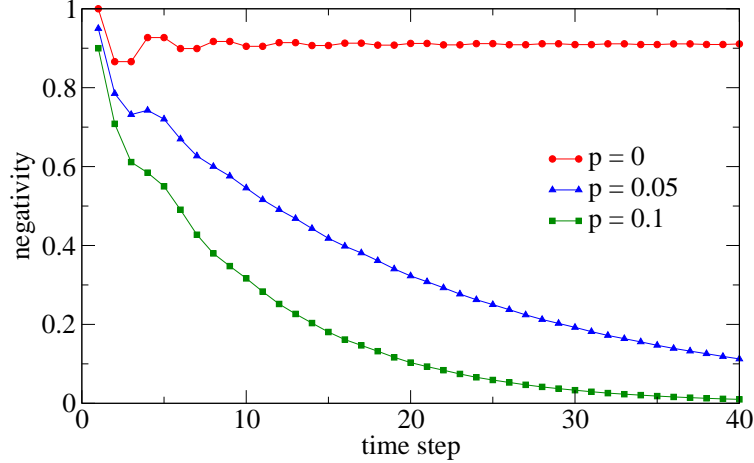


FIG. 4: Numerical data showing the negativity between the coin and position for decoherence rates $p = 0$ (red), $p = 0.05$ (blue) and $p = 0.1$ (green) for a quantum walk on the line with decoherence on both coin and position, run for 40 time steps.

computer with a single qubit for the coin and the position encoded in binary in the remainder of the quantum register. We perform a partial transpose on one subsystem to obtain a new matrix $\rho'(t)$. For example, the partial transpose with respect to the coin subsystem is

$$\rho'_{xc,yb}(t) = \rho_{xb,yc}(t) \quad (12)$$

where x, y are position indices and c, b are coin state indices. Next, we determine the spectrum of $\rho'(t)$, denoted by $\{\lambda'_i\}$. The normalisation of $\rho(t)$ is carried over to $\rho'(t)$, so $\sum_i \lambda'_i = 1$, but unlike $\rho(t)$, it is possible for $\rho'(t)$ to have negative eigenvalues. The negativity is defined [24, 25, 26] as

$$E = \frac{1}{2} \left(\sum_i |\lambda'_i| - 1 \right), \quad (13)$$

which is just the sum of the negative eigenvalues. The negativity ranges between zero and one, with any non-zero value indicating entanglement is present. If the negativity is zero, it means the state is probably not entangled, but there can be exceptions [27]. The exceptions are known to be relatively rare in the set of all possible states [28], and the entanglement they contain is difficult to apply to useful quantum tasks [27]. For this study, we will not need the fine-grained detail of these possible exceptions.

The entanglement in a pure state quantum walk has been studied previously, see for example, [29]. It fluctuates with each step, and eventually settles down to an asymptotic value that depends on the initial state of the quantum coin, and on any bias in the quantum coin operator \mathbf{C} . The addition of decoherence smooths out this behaviour, see figure 4, and steadily reduces the level of entanglement between the coin and the position.

II. RESULTS

Our simulations simply take equation (11) and evolve it numerically, calculating the negativity and, using an appropriate top hat or uniform distribution, the TVD for various types of decoherence

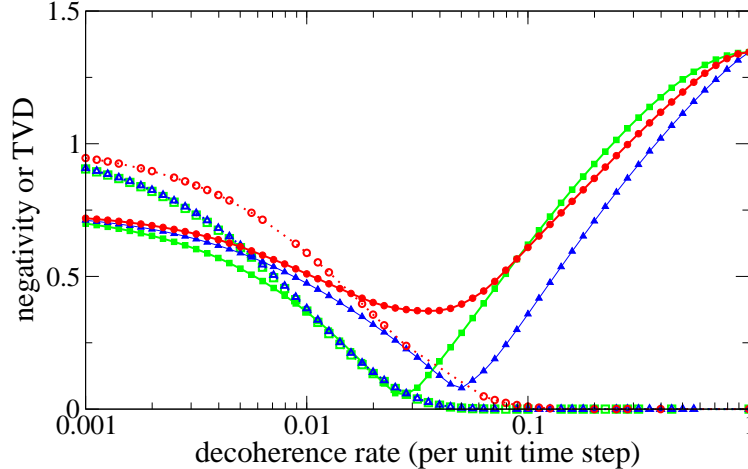


FIG. 5: Numerical data showing the negativity (dotted, open symbols) and TVD (solid, filled symbols) for decoherence applied to the position only (blue triangles), the coin only (red circles) and to both coin and position (green squares) for a quantum walk on the line of 100 steps. Some negativity data is missing (missing symbols).

and values of the decoherence rate p . We studied quantum walks on both the line and the cycle, for various initial states, lengths of walk, and sizes of cycles, with decoherence applied to the coin only, the position only, and to both the coin and position. These simulations can be accomplished on a desktop computer using straightforward code written in a language such as C++. We used various Apple Mac G4 and G5 computers and the versions of the GNU C compiler that come with the operating system OSX 10.4 and associated Developer Tools. Our results are summarised in the following subsections.

A. Entanglement in the walk on the line

Guided by the results in [14] and [29], we focused on the entanglement at the end of the quantum walk on the line, just before a final measurement would be made to find out where the quantum walker has ended up. We considered how the entanglement varies as the decoherence rate p is varied. As well as testing three cases of decoherence, applying it to both the coin and position, and also separately to just the coin or the position, we also tested two different starting states for the coin, both of which produce symmetrical distributions [21, 30], these being $(|-1\rangle + i|+1\rangle)/\sqrt{2}$ and $\cos(\pi/8)|-1\rangle + \sin(\pi/8)|+1\rangle$. The two initial states achieve a symmetrical distribution in fundamentally different ways, the former by combining two asymmetric distributions that do not interact, and the latter by arranging the interference exactly the right way to produce a symmetrical outcome. The distributions are not identical, and we observed that the TVD and negativity differ slightly, but not in any significant way. The negativity calculations require diagonalisation of large matrices (to find the eigenvalues), and we found for larger matrices (more time steps) our numerical routines (based on methods from Numerical Recipes [31]) did not always manage to do this. Failure was always reported by the routines, and we have simply left gaps in the figures where the negativity data is missing. We obtained sufficient results to show the overall trends, as can be

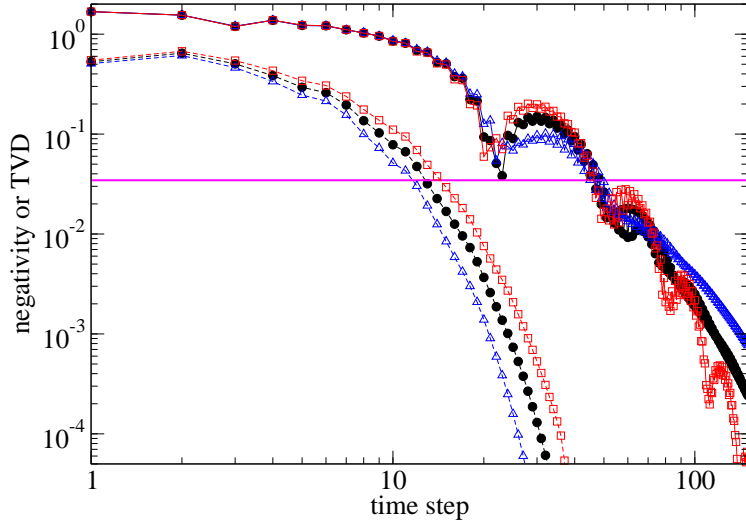


FIG. 6: Numerical data showing the negativity (dashed) and TVD (solid) for decoherence applied to the position for a quantum walk on the cycle of size 29 with $p = 0.2239$ (blue triangles), $p = 0.2511$ (black circles) and $p = 0.2818$ (red squares). The pink horizontal line is at $1/29$.

seen in a typical example from our results shown in figure 5. Both the TVD from the optimal top hat distribution, and the negativity are plotted. The minimum in the TVD indicates the optimal decoherence rate p . For a quantum walk of 100 steps the optimal p is in the range $0.025 \lesssim p \lesssim 0.05$. Note that the minimum for measurements on the coin only is much shallower. The distribution in this case retains a cusp shape [14]. The negativity is also higher than when decoherence is applied to the position of the walker, indicating that coin decoherence is less effective at removing the quantum correlations.

If decoherence is applied to the position, with or without decoherence on the coin as well, the negativity drops to zero at $p \simeq 0.055$, shortly after the optimal decoherence rate is reached. The optimal amount of decoherence is thus just about the amount required to remove the quantum correlations from the system. This makes intuitive sense: we are trying to achieve a uniform distribution on the line, in which any location within the top hat region is equally likely. Quantum correlations distort this smooth distribution, giving it peaks and troughs, especially at the ends of the top hat [1, 2]. If the decoherence rate is turned up until the classical random walk is obtained for $p = 1$, classical correlations build up to produce the binomial distribution in which the quantum walker is more likely to be found nearer the starting point of the walk. The fact that decoherence applied only to the coin does not produce a good top hat distribution shows that this result is non-trivial. There is no guarantee that decoherence can be arranged to remove the quantum correlations almost completely before any significant classical correlations build up, but for the quantum walk on the line it is possible to do this.

B. Entanglement in the walk on a cycle

For the mixing time on cycles, there are extra considerations. The mixing time depends not only on the size of the cycle, but also on how close to uniform one sets the threshold ϵ , see equations

(7) and (10). As already noted, pure quantum walks don't mix unless something is done to disrupt the pure quantum evolution. Both random decoherence and regular repeated measurements can efficiently change the behaviour into that of fast mixing to the uniform distribution. Note also that the optimal rate of measurement $2 \lesssim pN \lesssim 5$ is independent of the threshold ϵ , even though the main effect is to provide logarithmic scaling of the mixing time with ϵ .

We studied how the entanglement varies during the quantum walk on a cycle, with the decoherence rate p chosen to be near-optimal. As with the walk on the line, we examined the three cases of decoherence applied to both the position and coin, and applied to just the position or coin separately. Again decoherence applied to the coin only does not provide a significant improvement in the behaviour compared with decoherence applied to the position. The results for a typical example, a cycle of size $N = 29$ with decoherence applied to the position only, are shown in figure 6. While the actual mixing time is determined by the choice of ϵ , we have indicated the position of $1/N$ in figure 6, this being the probability of finding the walker at one location in a uniform distribution. The time at which the TVD drops below this line is around the time the entanglement also drops to zero. The variability of the TVD shows that the mixing time is not a smooth function of ϵ , so we cannot expect to determine a more precise result. As we argued for the walk on the line, quantum correlations are incompatible with the result we want, a uniform distribution, so the optimal quantum walk arranges for the quantum correlations to be removed by the end of the process.

C. Conclusion

The optimal quantum walk on the line and the cycle is a carefully balanced combination of quantum dynamics with decoherence or measurements providing randomness during the evolution of the walk. We have shown that, while the quantum correlations are necessary to obtain linear spreading and mixing times, they must be neutralised to produce a uniform final distribution.

Acknowledgments

We dedicate this paper to Ivens Carneiro, whose contribution to the work in [29] laid the foundations for these results. We learned with much sadness of his untimely death in a road accident in April 2006.

We also thank many other people for interesting discussions of quantum walks, among them, Hilary Carteret, Jochen Endrejat, Barbara Kraus, Peter Richter, Barry Sanders, Mario Szegedy, and Tino Tamon stimulated our thinking for the work in this paper. VK is funded by a Royal Society University Research Fellowship.

-
- [1] A. Ambainis, E. Bach, A. Nayak, A. Vishwanath, and J. Watrous, in *Proc. 33rd Annual ACM STOC* (ACM, NY, 2001), pp. 60–69.
 - [2] A. Nayak and A. Vishwanath (2000), extended abstract., quant-ph/0010117.
 - [3] Aharonov, D, A. Ambainis, J. Kempe, and U. Vazirani, in *Proc. 33rd Annual ACM STOC* (ACM, NY, 2001), pp. 50–59, quant-ph/0012090.

- [4] N. Shenvi, J. Kempe, and K. Birgitta Whaley, Phys. Rev. A **67**, 052307 (2003), quant-ph/0210064.
- [5] A. M. Childs, R. Cleve, E. Deotto, E. Farhi, S. Gutmann, and D. A. Spielman, in *Proc. 35th Annual ACM STOC* (ACM, NY, 2003), pp. 59–68, quant-ph/0209131.
- [6] A. Ambainis, in *45th Annual IEEE Symposium on Foundations of Computer Science, Oct 17-19, 2004* (IEEE Computer Society Press, Los Alamitos, CA, 2004), pp. 22–31, quant-ph/0311001.
- [7] J. Kempe, Contemp. Phys. **44**, 302 (2003), quant-ph/0303081.
- [8] B. C. Travaglione and G. J. Milburn, Phys. Rev. A **65**, 032310 (2002), quant-ph/0109076.
- [9] B. C. Sanders, S. D. Bartlett, B. Tregenna, and P. L. Knight, Phys. Rev. A **67**, 042305 (2003), quant-ph/0207028.
- [10] W. Dür, R. Raussendorf, V. M. Kendon, and H.-J. Briegel, Phys. Rev. A **66**, 052319 (2002), quant-ph/0207137.
- [11] D. Bouwmeester, I. Marzoli, G. P. Karman, W. Schleich, and J. P. Woerdman, Phys. Rev. A **61**, 013410 (1999).
- [12] V. M. Kendon and B. C. Sanders, Phys. Rev. A **71**, 022307 (2004), quant-ph/0404043.
- [13] C. A. Ryan, M. Laforest, J. C. Boileau, and R. Laflamme, Phys. Rev. A **72**, 062317 (2005), quant-ph/0507267.
- [14] V. Kendon and B. Tregenna, Phys. Rev. A **67**, 042315 (2003), quant-ph/0209005.
- [15] P. Richter, *Almost uniform sampling in quantum walks* (2006), ArXiv: quant-ph/0606202.
- [16] P. Richter, *Quantum speedup of classical mixing processes* (2006), ArXiv: quant-ph/0609204.
- [17] V. Kendon, Math. Struct. in Comp. Sci. (2007), To appear. ArXiv: quant-ph/0606016.
- [18] E. Farhi and S. Gutmann, Phys. Rev. A **58**, 915 (1998), quant-ph/9706062.
- [19] E. Bach, S. Coppersmith, M. P. Goldschen, R. Joynt, and J. Watrous, J. Comput. Syst. Sci. **69**, 562 (2004), quant-ph/0207008.
- [20] T. D. Mackay, S. D. Bartlett, L. T. Stephenson, and B. C. Sanders, J. Phys. A: Math. Gen. **35**, 2745 (2002), quant-ph/0108004.
- [21] B. Tregenna, W. Flanagan, R. Maile, and V. Kendon, New J. Phys. **5**, 83 (2003), quant-ph/0304204.
- [22] H. Krovi and T. A. Brun, Phys. Rev. A **74**, 042334 (2006), quant-ph/0606094.
- [23] T. A. Brun, H. A. Carteret, and A. Ambainis, Phys. Rev. A **67**, 032304 (2003), quant-ph/0210180.
- [24] A. Peres, Phys. Rev. Lett. **77**, 1413 (1996), quant-ph/9604005.
- [25] M. Horodecki, P. Horodecki, and R. Horodecki, Phys. Lett. A **223**, 1 (1996).
- [26] G. Vidal and R. F. Werner, Phys. Rev. A **65**, 032314 (2002), quant-ph/0102117.
- [27] M. Horodecki, P. Horodecki, and R. Horodecki, Phys. Rev. Lett. **80**, 5239 (1998), quant-ph/9801069.
- [28] K. Życzkowski, Phys. Rev. A **60**, 3496 (1999), quant-ph/9902050.
- [29] I. Carneiro, M. Loo, X. Xu, M. Girerd, V. M. Kendon, and P. L. Knight, New J. Phys. **7**, 56 (2005), quant-ph/0504042.
- [30] N. Konno, Quantum Information Processing **1**, 345 (2002), quant-ph/0206053.
- [31] W. H. Press, B. P. Flannery, S. A. Teukolsky, and W. T. Vetterling, *Numerical Recipes in C (2nd Edition)* (Cambridge University Press, 1993).